

Original article

Numerical evaluation of hydrogen production by steam reforming of natural gas

Mingjie Chen¹*, Khalid Al-Subhi^{2,3}, Amira Al-Rajhi¹, Ali Al-Maktoumi^{1,4}, Azizallah Izady¹, Amer Al-Hinai⁵

¹Water Research Center, Sultan Qaboos University, Muscat 123, Oman

²Sustainable Energy Research Center, Sultan Qaboos University, Muscat 123, Oman

³Department of Chemical and Biological Engineering, The University of Sheffield, Sheffield S13JD, UK

⁴Department of Soils, Water and Agricultural Engineering, Sultan Qaboos University, Muscat 123, Oman

⁵Department of Electrical and Computer Engineering, Sultan Qaboos University, Muscat 123, Oman

Keywords:

Hydrogen production
combustor
steam methane reforming
shift reactor
Aspen HYSYS
response surface

Cited as:

Chen, M., Al-Subhi, K., Al-Rajhi, A., Al-Maktoumi, A., Izady, A. Al-Hinai, A. Numerical evaluation of hydrogen production by steam reforming of natural gas. *Advances in Geo-Energy Research*, 2023, 7(3): 141-151.

<https://doi.org/10.46690/ager.2023.03.01>

Abstract:

Industry-scale hydrogen is mainly produced by steam methane reforming (SMR), which uses natural gas as the feedstock and fuel and co-produces CO₂. This study aims to numerically evaluate hydrogen production by SMR under various reacting conditions. Unlike the previous studies with limited scenarios, the performance of SMR is continuously evaluated in a high-dimensional input-parameter space. The SMR plant including a combustor, a reformer, and a water-gas shifter is modeled in Aspen HYSYS software. The four key parameters, including methane fraction of the feedstock, reformer pressure and temperature, and shifter temperature, are treated uncertain and 50 samples are drawn from a four-dimensional parameter space defined by their ranges. Each sample is input to HYSYS model and mass ratio of each component in product streams is obtained as the output variables. Based on the 50 pairs of input-output data, response surfaces of the outputs are developed to surrogate HYSYS models. The fast response surface models are then used to calculate global sensitivity indices and evaluate SMR processes. Results show the reformer performance is controlled by temperature rather than pressure, and a temperature higher than 900 °C can maximize the reaction rate. The water-gas shifting reaction is inhibited in the reformer but significantly enhanced in the shifter. Hydrogen is mainly produced in the reformer while the major function of the shifter is to convert CO to nontoxic CO₂.

1. Introduction

In the past decades, molecular hydrogen (H₂) has been receiving rising attentions as a clean, safe fuel and energy carrier. It can be stored for a long term and transported over long distances with minor losses, allowing the storage and distribution of energy between countries (Ball and Weeda, 2015; Zhang et al., 2022). Hydrogen production can be considered as a process transforming it from its compound by using other energy sources, so it is a kind of energy carrier to move, store, and deliver energy from other sources (Hermesmann and Müller, 2022; Scovell, 2022). It hence is

considered as the solution to global energy and environmental problems by replacing the current fossil fuel system with the new hydrogen energy system (Veziroglu and Sahin, 2008; Yue et al., 2021; Zhang et al., 2023). Many oil-producing countries, including Oman, are implementing a long-term strategic policy to establish hydrogen energy system in order to diversify their petroleum-dominated economy for sustainable development (Ansari, 2022) Although hydrogen is the most abundant element in universe, it rarely exists alone naturally on Earth. Most of hydrogen on earth exists in biomass, water (H₂O), methane (CH₄), coal, and petroleum, from which H₂

can be produced (Seyitoglu et al., 2017; Inayat et al., 2020; Hjeij et al., 2022). To date, steam methane reforming (SMR) is the most economic and primary method for H₂ production. Natural gas is used as both raw material and burning fuel in SMR process with byproduct CO₂ (Mokheimer et al., 2015). Around 5% of global H₂ production is made from water electrolysis, in which H₂O is used as raw material and electricity as energy source (Ulleberg, 2003). As fossil fuel is the primary energy to generate electricity, hence water electrolysis could also indirectly produce CO₂. Green H₂ produced by water electrolysis using electricity generated by non-carbon energy sources, including solar, wind, and geothermal has been extensively studied and implemented (Balta et al., 2010; Bicer and Dincer, 2016; Mostafaeipour et al., 2016; Saleem et al., 2020). Particularly, integrated solar-electrolyzer systems are well developed and commercially available now. Whereas, before the complete transition to green H₂ production, SMR would still be the most important hydrogen production method to meet the global hydrogen demand for a long time.

The steam-reforming reactor has been studied using various modeling approaches. Mokheimer et al. (2015) designed a reformer unit and developed a dynamic computational fluid dynamics (CFD) model verified by experiment data. The impacts of operational parameters are investigated. They found that decrease of pressure and increase of the ratio of steam to the methane favor higher conversion rate. Similar CFD modeling work by Chiu et al. (2019) showed that methane conversion and hydrogen production raised when temperature increase. High flow rate of the feedstock leads to decrease in the conversion, and longer catalyst bed yields higher conversion. Pourali et al. (2021) developed an analytical model to simulate microscale-reforming reactor. Their results show both CH₄ conversion and CO₂ selectivity linearly change with temperature. Peng and Jin (2022) conducted a molecular simulation of the reforming reaction, and demonstrated that the conversion calculated from Gibbs energy of formation matches the data from Chemeq program (Sandler, 1999).

While the above modeling studies are focused on the reforming reactor only, several researchers evaluated SMR plant system consisting of multi-stage multi-reactors. Cancela et al. (2015) designed a SMR plant with four reactors, including a combustor, a reformer, a water-gas shifter, and a selective oxidation of CO, and modeled the system using Matlab Simulink module (Mathworks, 2022). They concluded that the efficiency of overall methane conversion depends on steam-methane ratio and the most efficient ratio is 3:1. Hoeghian et al. (2018) performed a steady-state simulation and optimization for a SMR plant including reforming, shifting, amine, and separating units. An optimal set of operational parameters, including steam-methane ratio, reformer temperature, pressure, and shifter temperature, were obtained. The main limitation of these studies is that the analysis is based on a couple of scenarios, and fails to track response of SMR performance to the continuous changes of the multiple operational conditions. To meet this need, we apply the response surface (RS) method to evaluate a SMR plant system in a continuous multi-dimensional input parameter space. Response surface, or surrogate model, is a kind of data-driven model to approximate

a physics-based model for fast predictions (Razavi et al., 2012; Chen et al., 2022). The fitted RS model should be validated to ensure acceptable accuracy before prediction.

In this study, RS models are developed using the dataset from Aspen HYSYS process models (AspenTech, 2022). Firstly, a set of operational parameters are sampled in a multi-dimensional input parameter space constrained by specified ranges. Secondly, the input samples are used to develop a suite of HYSYS models. Thirdly, RSs between the key input parameters and performance indicators are constructed and validated using the dataset from HYSYS model simulations. Lastly, the developed RSs are used for global sensitivity analysis and evaluations of the SMR plant performances in response to the set of input parameters.

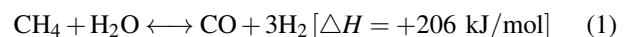
2. Modeling methods

2.1 Steam reforming plant model

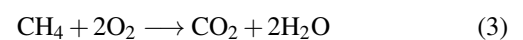
Aspen HYSYS, a premier hydrocarbon process simulation software, is used to develop a steam reforming plant model simulating hydrogen production by SMR. As shown in Fig. 1, the chemical plant includes a combustor to burn natural gas to provide heat for the reforming process, a reformer to produce syngas, and a water-gas shifter to increase hydrogen yield. The terms in Fig. 1 are described in Tables 1 and 2. The product stream should be sent to an amine unit to separate CO₂ from the sweet gas, which comprises carbon monoxide (CO), steam, hydrogen, and unreacted methane. The sweet gas should also be further processed in a methanation unit to convert toxic CO to nontoxic product. The amine and methanation units are not included in the processing flowchart since they are beyond the scope of this study.

To facilitate the basis of the study, a few assumptions on the reactors are made as follows: (1) Reforming and shifting reactions are assumed isobaric and equilibrium, and governed by Peng-Robinson equation of state, (2) The reformer is isothermal and thus experiences no temperature change (3) The feed of methane and oxygen to the combustor are constant regardless of the conditions of the SMR system. Although pure oxygen is fed to the combustor unit in the design, an air mixture will be used containing an approximate of 7% nitrogen with a balance of oxygen in reality. Oxygen is supplied in 17.5% excess for the combustion reaction.

The binary mixture of steam and methane is heated to a specific temperature and fed into the reformer unit where the following reversible reactions occur in series:



Since the reforming process is strongly endothermic, the required heat are provided by the product stream of a methane combustion reaction (Fig. 1). Since oxygen is supplied in excess, it is assumed that complete combustion is achieved as per the following irreversible reaction:



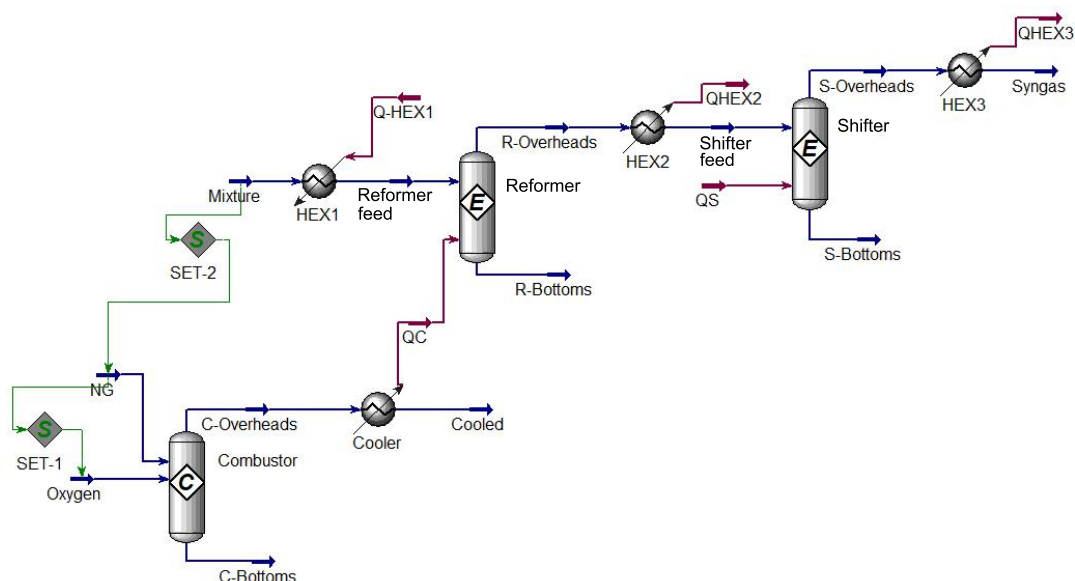


Fig. 1. Flowchart of the Aspen HYSYS model simulating steam reforming of national gas. The equipment and stream terms are described in Tables 1 and 2.

Table 1. Descriptions of equipments in the flowchart of hydrogen production shown in Fig. 1.

Equipment identifier	Description	
Reactors	Reformer	The equilibrium reformer reactor
	Shifter	The equilibrium shift reactor
	Combustor	The combustion reactor
Heat exchangers	HEX1	The unit heating the feedstock to the reformer
	HEX2	The unit cooling down the products from the reformer
	HEX3	The unit cooling down the products from the shifter
	Cooler	This unit supplying heat from the combustor to the reformer

The outlet stream of the reformer, including left CH_4 , CO_2 , CO , H_2 , and H_2O , are fed into the subsequent shifting reactor, where H_2 composition is further elevated by the reaction of Eq. (2). The reaction of Eq. (1) is neglected in the shifter as the temperature is relatively low. As a result, CH_4 composition remains unchanged between the inlet and outlet of the shifter.

Two sets are specially designed to facilitate the reforming processes (Fig. 1): (1) SET-1 ensures that oxygen is supplied in 17.5%-excess regardless of the variation in masses of feedstock, and (2) SET-2 allocates constant flow of methane to the combustor. It may be noteworthy to mention that the heat discharged from the reformer may be used for additional heating purposes.

Aspen HYSYS handles phase transitions where applicable and apply the changes necessary to the vapor/liquid system according to its embedded Peng-Robinson equation of state. Nonetheless, the binary feedstock mixture of methane and water in this study has a relatively low boiling point and hence it is 100% vapor once heated to the reformer temperature in the unit HEX1 (Fig. 1). Similarly, the products and by-products of CO , CO_2 , and H_2 also have low boiling points. Therefore, the

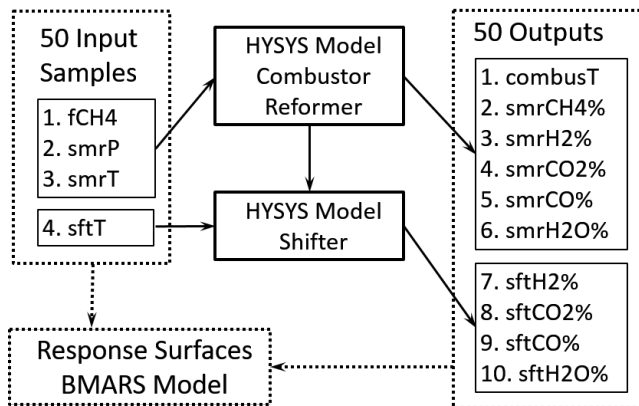
only stream that phase transition may occur in is the product of the cooler HEX3 (Fig. 1), the feed to the amine separation unit, which is excluded from the simulation. HEX3 would cool the process stream to temperatures below 100°C prior to the separation of CO_2 from the other components.

2.2 Response surface model

To evaluate the steam reforming process with continuously varying conditions, including feedstock composition, reactor pressure and temperature, RS models of performance metrics in the four-dimensional (4-D) input parameter space are developed based on 50 HYSYS model simulations. As shown in Fig. 2, four input parameters, including f_{CH_4} , smrP , smrT , and sftT , are considered key factors. Total 50 samples are uniformly drawn from a 4-D parameter space constraint by these four parameter ranges using Latin Hypercube method (McKay et al., 1979). The description of the four parameters along with their ranges are presented in Table 3. Obviously, sftT is only involved in the shifting reaction, while f_{CH_4} , smrP , and smrT affect the reformer, as well as the subsequential shifter. In addition to the four uncertain inputs, the methane

Table 2. Descriptions of material/energy streams in the flowchart of hydrogen production shown in Fig. 1.

	Stream identifier	Description
SMR material	Mixture	A binary mixture of steam and methane
	Reformer feed	Heated mixture feedstock to the reformer
	R-Overheads	Gaseous products of the reformer
	R-Bottoms	liquid product of the reformer
	Shift feed	Gaseous feedstock to the shifter
	S-Overheads	Gaseous products of the shifter
	S-Bottoms	Liquid products of the shifter
	Syngas	Cooled gaseous products from the shifter
SMR energy	QHEX1	The heat duty supplied to heat the binary feed mixture
	QHEX2	The heat duty removed from the reformer products
	QHEX3	The heat duty removed from the shifter products
	QC	The heat duty from the combusted gas to the reformer
	QS	The heat duty required for the shifter
	QA	The heat duty required for the amine separation unit
Combustor material	NG	Natural gas as the fuel for combustion
	Oxygen	Oxygen stream for the combustion of methane
	C-Overheads	Gaseous products from the combustor
	C-Bottoms	Liquid products from the combustor
	Cooled	Cooled products from the reformer

**Fig. 2.** Flowchart of response surface method in this study. The input and output parameters are described in Tables 3 and 4.

and steam mixture flow fed to the reformer is fixed as 21.99 kg/s. Methane and air mass to the combustor is specified as 2.61 and 58.18 kg/s, respectively. The total mass flow to the plant system amounts to 82.78 kg/s.

As shown in Table 4, 10 indicators derived from model outputs are designed to evaluate the reactors performance. combustT represents the temperature of the stream out of the combustor exchanger, which supplies heat generated from the combustion reaction to the reformer. It measures the heat consumption by the reforming reaction. The lower the comb-

Table 3. The 4 uncertain input parameters and their ranges. Mass flow rate is fixed as 22 kg/s.

Name	Description	Range
fCH4	Methane fraction in the feedstock mixture (mol/mol)	0.2-0.35
smrP	The reforming reactor pressure (kPa)	200-1,000
smrT	The reforming reactor temperature (°C)	600-1,200
sftT	The shifting reactor temperature (°C)	250-600

ust, the more the heat consumed. smrCH4% denotes the mass percentage of CH₄ in the stream out of the reformer. Similarly, smrH2%, smrCO2%, smrCO%, and smrH2O% are mass percentages of the respective gas at the reformer outlet, while sftH2%, sftCO2%, sftCO%, and sftH2O% are the counterparts at the shifter outlet. Note CH₄ composition at the shifter outlet is the same as smrCH4%.

Bagging multivariate adaptive regression spline (BMARS) is the bootstrap expectation of multivariate adaptive regression spline (MARS) model ensemble, which ensures more stable and reliable predictions (Bühlmann, 2003). Detailed theory of the MARS algorithm can be found in Friedman (1991). Chen et al. (2013, 2020) applied BMARS to approximate a hydro-fracking model and a CO₂-brine flow model successfully. In this study, BMARS algorithm is used to develop RS models

Table 4. Description of the 10 outputs of the combustor, reformer, and shifter models.

#	Name	Description
1	combustT	Temperature of post-combustor stream (°C)
2	smrCH4%	The reformer CH ₄ mass percentage
3	smrH2%	The reformer H ₂ mass percentage
4	smrCO2%	The reformer CO ₂ mass percentage
5	smrCO%	The reformer CO mass percentage
6	smrH2O%	The reformer H ₂ O mass percentage
7	sftH2%	The shifter H ₂ mass percentage
8	sftCO2%	The shifter CO ₂ mass percentage
9	sftCO%	The shifter CO mass percentage
10	sftH2O%	The shifter H ₂ O mass percentage

of the 10 performance indicators to the four input parameters of the HYSYS model. The fitted RS models are validated using the leave-one-out cross-validation method (Picard and Cook, 1984), in which the RS model is fitted 50 times, each time using 49 samples, and the excluded sample is used to test how well the RS predictions match the HYSYS model data.

2.3 Global sensitivity analysis

Sobol' total-order index (STI) can be used to measure the sensitivity of each output to input parameters (Sobol', 2001). It entails a large number of model runs, but can be efficiently accomplished using the developed RS models (\hat{f}). The sensitivity indices (SI) and STI can be expressed as following equations:

$$SI_i = \frac{\text{Var}[E(\hat{f} | x_i)]}{\text{Var}(\hat{f})} \quad (4)$$

$$SI_{ij} = \frac{\text{Var}[E(\hat{f} | x_i, x_j)] - \text{Var}[E(\hat{f} | x_i)] - \text{Var}[E(\hat{f} | x_j)]}{\text{Var}(\hat{f})} \quad (5)$$

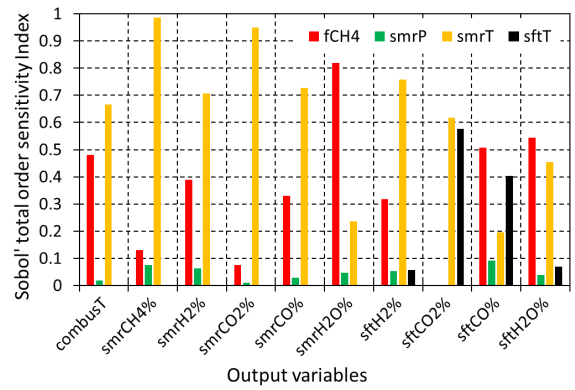
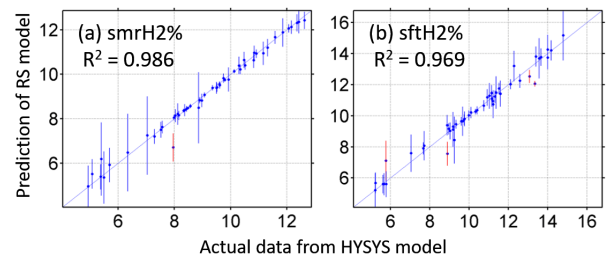
$$STI_i = SI_i + \sum_{j \neq i} SI_{ij} + \sum_{j \neq i, k > j} \sum SI_{ijk} + \dots \quad (6)$$

where SI_i is the 1st order sensitivity of input variable x_i , SI_{ij} is the 2nd indices of x_i and x_j , measuring the contribution of the interactions of between the two parameters to the variances. SI_{ijk} is the third-order indices, and STI_i is the total-order Sobol' sensitivity indices of x_i .

STI represents the total contribution of each input parameter to the output variances, including its interactions with other parameters in all the orders. STI varies between 0 and 1, and parameters with $STI > 0.05$ are considered sensitive in this study and included for global sensitivity analysis.

3. Results and analysis

The quality of RS models are examined by comparing their predictions to the HYSYS models. Fig. 3 presents the validation results for RS of smrH2% and sftH2%. The 0.986 and 0.969 of R_2 values for the two scatterplots suggest that

**Fig. 3.** Sobol' total order sensitivity indices of the 10 model outputs to the 4 input parameters.**Fig. 4.** Validation of response surface models fitted by BMARS: (a) smrH2% of the reforming reactor, and (b) sftH2% of the shifting reactor. The red lines denote the predictions are outside of ± 1 standard deviation.

the two RS models can well surrogate the respective HYSYS models. Both mean and ± 1 standard deviation of the ensemble MARS outputs of each BMARS model are shown in the scatterplots. In the following sub-sections, SMR performance is evaluated using STI (Fig. 4), visualized two-dimensional (2-D) RSs of the performance indicators to sensitive parameters ($STI > 0.05$) (Figs. 5-9), and their relationships (Fig. 10).

3.1 combust

According to the STI presented in Fig. 4, combustT is sensitive to fCH4 and smrT, and its RS to the two sensitive parameters is visualized in Fig. 5. It shows that combustT is negatively correlated to both fCH4 and smrT in general. Moreover, smrT dominates combustT in the low smrT area (< 900 °C), while fCH4 starts to take control of combustT in the high area. According to the definition of combustT, a lower value indicates more heat is consumed by a higher reforming reaction rate. The results suggest that favorable temperature for reforming reactor should be below 900 °C for best cost-efficiency, as the reaction cannot be enhanced any more by the temperature when it is higher than 900 °C.

3.2 smrCH4%

smrCH4% is dominantly affected by smrT ($STI = 0.986$), and slightly by fCH4 ($STI = 0.131$) and smrP ($STI = 0.075$). RSs in response to two parameter pairs between the top-sensitive parameter and the other two, i.e., fCH4-smrT, and

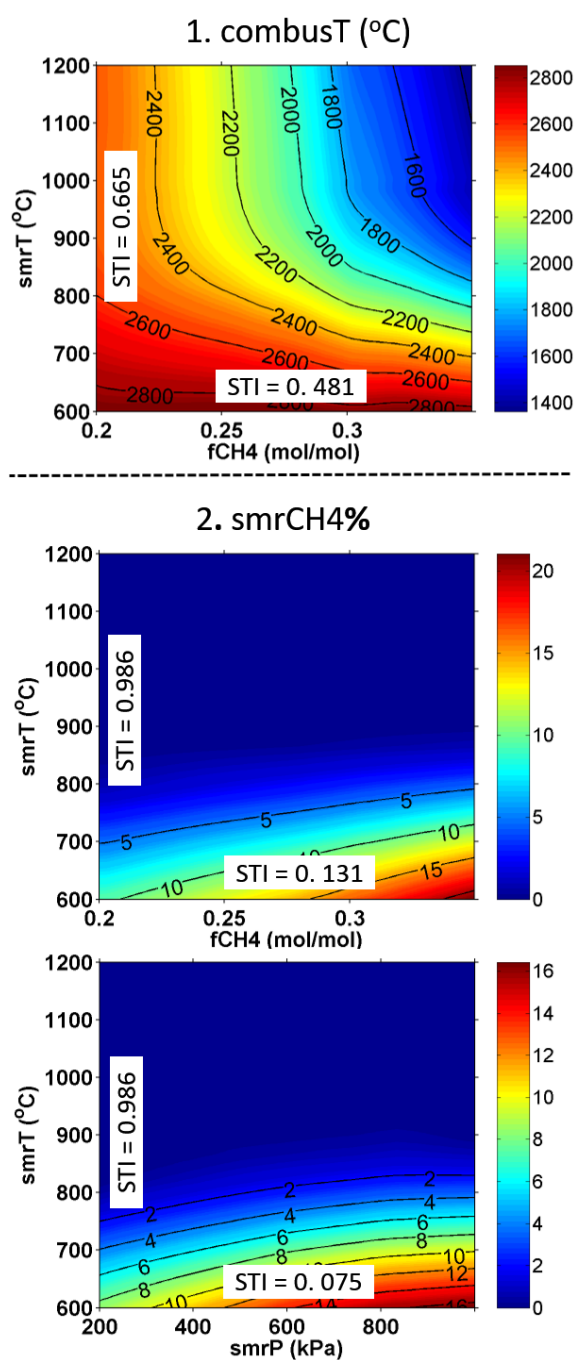


Fig. 5. 2-D response surfaces of combustT (output# 1) and smrCH4% (output# 2) to their sensitive input parameters (STI > 0.05).

smrP-smrT, are visualized in Fig. 5. It shows smrCH4% decreases with the increase of smrT to nearly zero at 900 °C. The result suggests high temperature can enhance CH₄ conversion, but it is unnecessary to be above 900 °C. Besides, in smrT < 900 °C area, the outlet mass fraction of CH₄ (smrCH4%) is almost linearly and positively correlated to inlet fraction (fCH4), which is expected for an equilibrium reaction. Similar to fCH4, smrP affects smrCH4% very slightly in the low smrT area, and lower smrP seems to facilitate reforming reaction.

3.3 smrH2% and sftH2%

The RSs of both smrH2% and sftH2% in response to fCH4 and smrT (Fig. 6) show a reversed pattern compared to that of combustT. It is expected as a higher reforming rate consumes more heat, leading to a lower combustT. The RSs also confirm that above 900 °C, hydrogen production can only be promoted by feeding more methane (fCH4). The impact of smrP on smrH2% or sftH2% is nearly negligible (STI = 0.064 or 0.052). It is seen that sftH2% is strongly sensitive to the reformer temperature (smrT) and methane feedstock to the reformer (fCH4), showing similar RS patterns as smrH2%. However, it is almost insensitive to the shifter temperature (sftT, STI = 0.056). The results suggest that sftH2% depends mainly on the stream flow from the reformer, and the impact of shifter temperature on the shifting reaction is almost negligible in its specified range. Besides, sftH2% is elevated from smrH2% by 10%-20% in various reformer conditions, as partial CO and steam in the reformer syngas are converted to H₂ and CO₂ in the shifter.

3.4 smrCO2% and sftCO2%

Although CO₂ is a coproduct of H₂ from the reforming reaction, its RS shows a completely different distribution pattern from that of H₂ (Fig. 7). smrCO2% is dominated by smrT (STI = 0.948), and only affected by fCH4 slightly (STI = 0.075). Moreover, it monotonously decreases with the increase of smrT in its full range of 600-1,200 °C. As concluded from the above analysis on combustT and smrH2%, smrT higher than 900 °C won't affect H₂ production and associated heat consumption. According to Eqs. (1) and (2), H₂ is mainly produced by reaction 1, which is strongly endothermic, while CO₂ is only produced by reaction 2, which is slightly exothermic. As such, high smrT will promote H₂ production by reaction 1 but inhibit CO₂ production by reaction 2.

sftCO2% is almost equally sensitive to smrT and sftT with respective 0.617 and 0.577 of STI, and insensitive to fCH4 or smrP. The RS in response to the two sensitive parameters are shown in Fig. 7 (right). sftCO2% is negatively correlated to sftT, since reaction 2 happened in the shifter is a slightly exothermic reaction. In contrast to smrCO2%, sftCO2% is positively correlated to smrT. Particularly in 600-800 °C range, sftCO2% rises sharply from 35% to over 55% at sftT = 200 °C, while smrCO2% remains almost constant at 22%. The comparison of smrCO2% and sftCO2% strongly demonstrates how high temperature could inhibit CO₂ production by reaction 2, which happens in both reformer and shifter. As temperature falls from smrT (600-1,200 °C) to sftT (200-600 °C), CO₂ percentage is elevated by up to fivefold. CO₂ mass percentage remains almost the same at 22% from the reformer to the shifter when both smrT and sftT equal 600 °C (Fig. 7).

3.5 smrCO% and sftCO%

CO is produced during reforming reaction (Eq. (1)), and a small portion is converted to CO₂ in the reformer (Eq. (2)). It is more significantly reacted with H₂O to form CO₂ in the shifter at a lower temperature of sftT than smrT. The RS of smrCO% in response to the controlling parameters fCH4 and smrT is

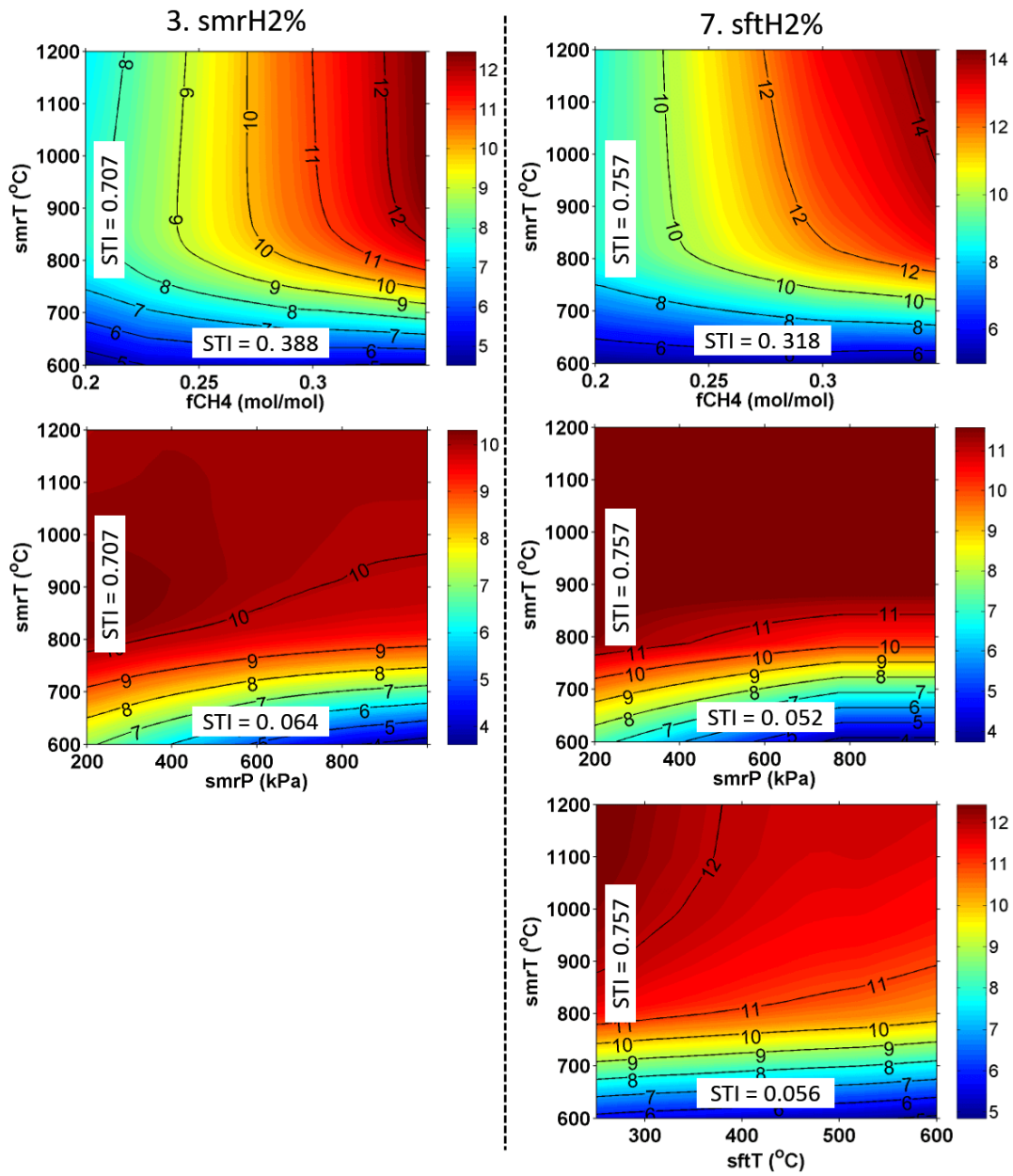


Fig. 6. 2-D response surfaces of of smrH2% (output# 3) and sftH2% (output# 7) to their sensitive input parameters (STI > 0.05).

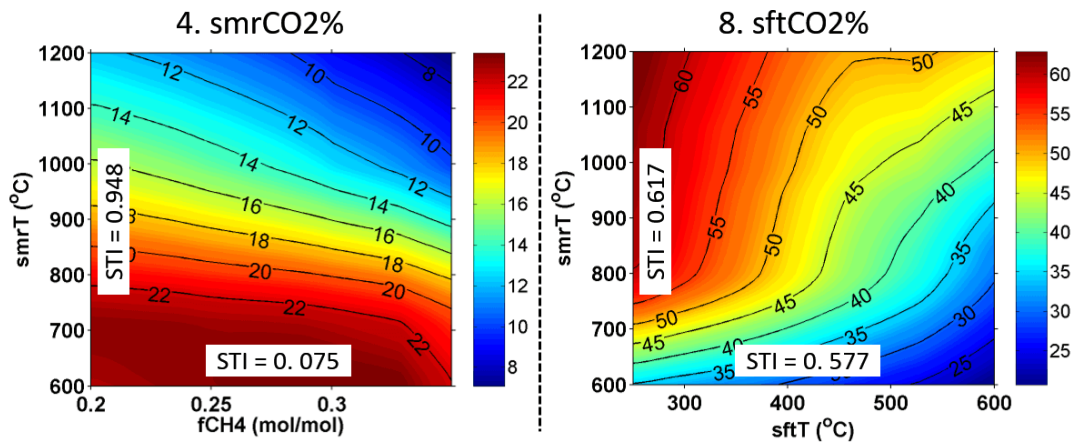


Fig. 7. 2-D response surfaces of smrCO2% (output# 4) and sftCO2% (output# 8) to their sensitive input parameters (STI > 0.05).

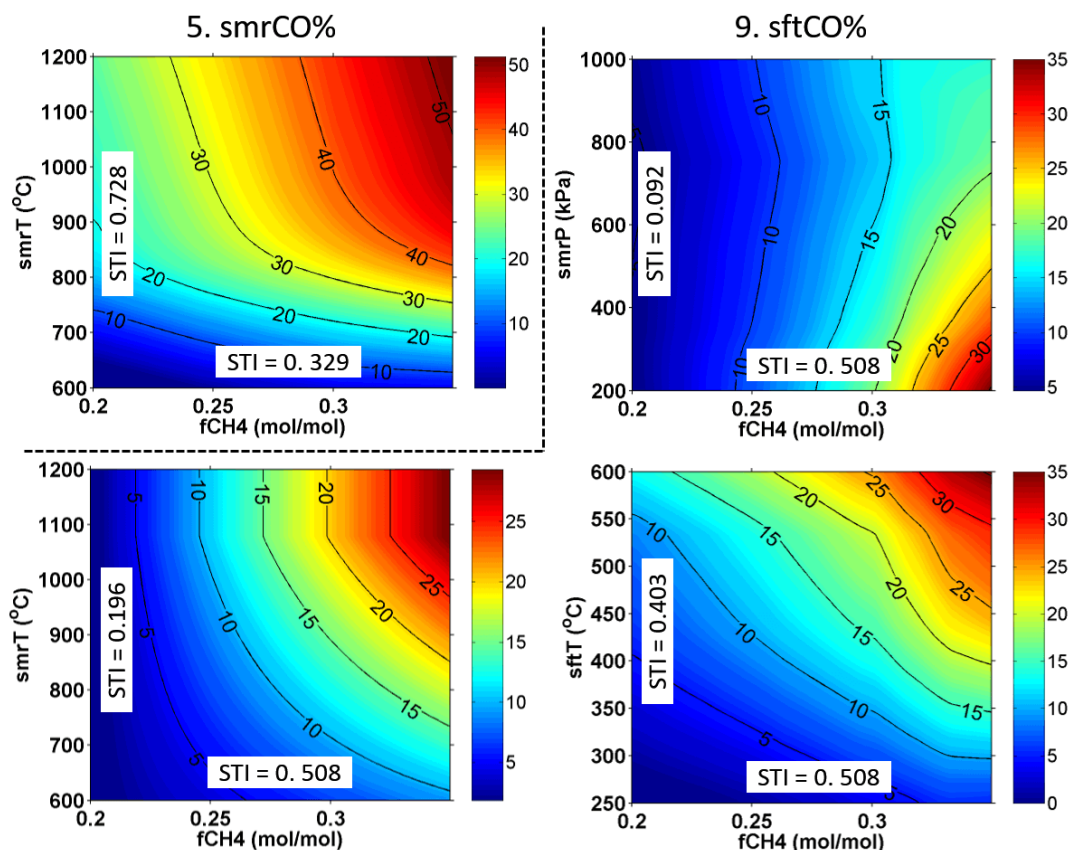


Fig. 8. 2-D response surfaces of of smrCO% (output# 5) and sftCO% (output# 9) to their sensitive input parameters (STI > 0.05).

presented in Fig. 8 (top left). Similar to smrH2%, it is strongly affected by smrT at low smrT (< 900 °C), but by fCH4 instead at high smrT. However, smrCO% is also moderately impacted by smrT above 900 °C, continuing to increase with smrT, but in a more slow rate in this high temperature range. This behavior of smrCO is different from its coproduct H₂ of the reaction 1. It is because CO could be reversely generated from CO₂ in reaction 2 at high smrT, since Eq. (2) is a reversible exothermic reaction. The decrease of smrCO₂% accounts for the increase of smrCO% in this smrT range.

All the four input parameters affect sftCO% more or less, and three RSs between the top sensitive fCH4 and the other three parameters are visualized in Fig. 8, along with one RS of smrCO%. It is found that sftCO% is reduced from smrCO% by about half. It is positively correlated to sftT, as high temperatures prevent CO from conversion to CO₂ by reaction 2 in the shifter.

3.6 smrH2O% and sftH2O%

As one of the raw materials, steam is consumed to produce hydrogen in both Eqs. (1) and (2). The RS of smrH2O% in response to fCH4 and smrT shows an opposite distribution to that of smrH2% (Fig. 9). It is more strongly sensitive to fCH4 but less to smrT than smrH2%. Stream fraction is reduced in the shifter, as more H₂O is converted to H₂ according to reaction 2. sftH2% is slightly increased with the increase of sftT (STI = 0.07), as high temperature would inhibit reaction

2. Similar to sftH2%, sftH2O% depends primarily on streams from the reformer, instead of the shifter temperature.

3.7 Relationships between outputs

To further investigate the interactions between the combustion, reforming and shifting reactors, probability histograms of the 10 outputs from the 50 simulations, as well as their pairwise joint probability, are plotted in Fig. 10. The sub-figures contained in the upper and lower triangles and the square delineated by red dashed lines show the interactions between the three reactors, as well as relationships between chemicals in the reformer (output# 3-6) or the shifter (output# 7-10). For the sake of convenient description, we define the location of a joint probability (JP) in Fig. 10 as JPXY, where X and Y denote output number in X and Y axis, respectively. For example, JP32 stands for the joint probability between output# 3 in X (smrH2%) and 2 in Y (smrCH4%).

As shown in JP31 and JP51, combust is almost linearly negative-correlated to smrH2% and smrCO%, suggesting the heat consumed in reaction 1 is proportional to the production of H₂ and CO. It is positively correlated to smrH2O% (JP61), as both heat and steam are consumed in reaction 1. combust is roughly positive-correlated to smrCO₂% (JP41), because both of them are negatively correlated to smrT. A higher smrT will enhance reaction 1 yielding a lower combust, and inhibit reaction 2 producing less to CO₂.

Output# 2-6 include the five reactants in the reformer. Am-

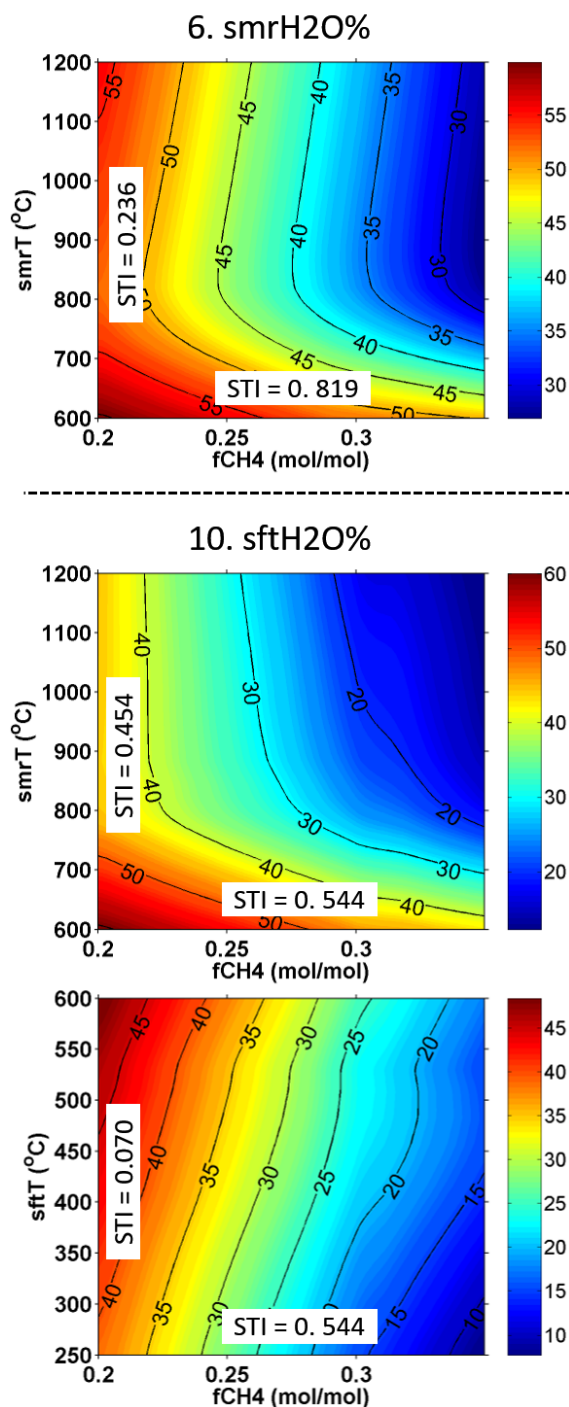


Fig. 9. 2-D response surfaces of of smrH2O% (output# 6) and sftH2O% (output# 10) to their sensitive input parameters (STI > 0.05).

ong them, CH₄ and H₂O are converted to CO and H₂, and partial CO is further converted to CO₂. According to smrCH₄% probability histogram (JP22), CH₄ is completely consumed in more than 50% of the 50 simulations, and smrCH₄% of the left simulations is relatively evenly distributed between 2-18 percentage. As the product of the major reaction 1 in the reformer, H₂ and CO is strongly positive-correlated to each other (JP53), and both of them are negatively correlated to the feedstock H₂O (JP63 and JP65). As for CO₂, it is

produced from CO by the minor reaction 2. However, the CO consumed in reaction 2 is negligible compared to CO produced in reaction 1. As the influence of smrT on reaction 1 and 2 is opposite, smrCO₂% generated by reaction 2 is negatively correlated to smrCO% (JP54) or smrH₂% (JP43) by reaction 1. The opposite impact of smrT on reaction 1 and 2 also explains the weakly positive correlation between smrCO₂% and smrH₂O% (JP64).

The diagonal JPs of the square area outlined by the red dashed represent the correlations for each of H₂, CO₂, CO, and H₂O between the reformer and shifter. The strong positive-correlations of H₂ (JP73) or H₂O (JP106) between the two reactors suggest the reforming process dominates the final fraction of the two components, rather than the shifting reaction. In contrast, no apparent correlation is found for CO₂ percentage (JP84). The JP95 for CO shows a upper triangle distribution, indicating large values of smrCO% is reduced to low percentage as sftCO%. This result suggests CO is significantly reduced by conversion to CO₂ in the shifter.

The JPs between H₂, CO₂, CO, and H₂O may change significantly from the reformer to the shifter, except those between H₂ and H₂O. Both JP63 and JP107 show a similar strong negative-correlation, as H₂O is consumed to produce H₂ in both reformer and shifter. On the contrary, the negative correlation between smrH₂% and smrCO₂% (JP43) becomes positive between sftH₂% and sftCO₂% (JP87). It is because in the shifter, both H₂ and CO₂ are the final products of the single reaction (Eq. (2)). Similar to JP95, high probabilities are distributed on left upper triangle of JP97 (sftH₂% and sftCO%), because substantial CO is converted. No obvious correlation is identified between sftCO₂% and sftCO% (JP98). In contrast to rough positive-relationship in the reformer (JP64), sftCO₂% is found to be negatively correlated to sftH₂O% (JP108), as H₂O is consumed in the shifter. The negative correlation between smrCO% and smrH₂O% (JP65) is shifted to a left lower triangle distribution in its counterpart of the shifter (JP109), as CO is significantly reduced in most of the 50 simulations.

4. Summary and conclusions

A model for steam methane reforming plant consisting of a combustor, a reformer and a shifter is developed using Aspen HYSYS, and its performance is evaluated using response surface method. A set of performance indicators of the three reactors are assessed for four key input parameters, including post-combustor temperature, reformer temperature and pressure, and shifter temperature. Major conclusions are summarized below:

- Temperature is the dominant factor controlling the reforming reaction (Eq. (1)), which is restricted by a temperature < 900 °C. However, the reforming process would be limited by availability of methane instead in the range of 0.2-0.35 mole fraction if given a temperature higher than 900 °C.
- The water-gas shifting reaction (Eq. (2)) happens in both reformer and shifter, but it is strongly inhibited by the high temperature in the reformer (600-1,200 °C). The reaction is significantly enhanced in the shifter with lower

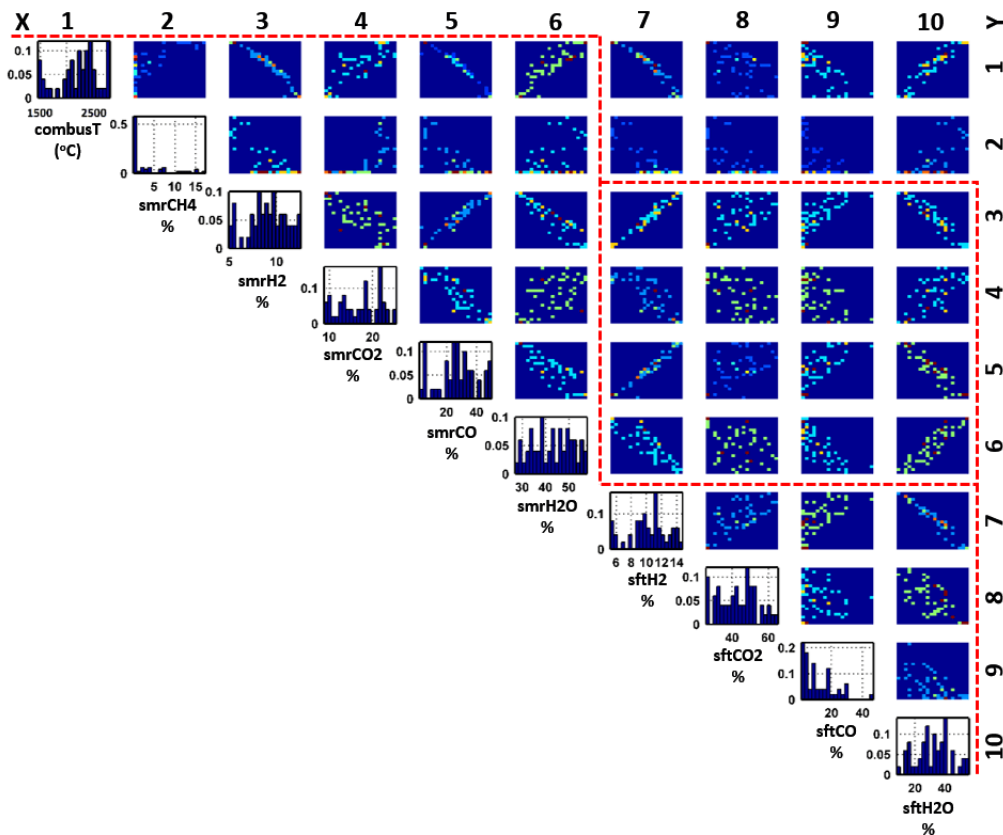


Fig. 10. Histograms and 2-D joint probability distributions between the 10 outputs.

temperature (200-600 °C). The reformer pressure shows negligible impact on the reforming process in its range of 200-1,000 kPa.

- The temperature play a major role in CO and CO₂ compositions out of the shifter. H₂ or H₂O composition, however, is insensitive to the reaction temperature in the shifter, but primarily affected by the streams from the reformer. Hydrogen production is mainly contributed by the reformer, while converting toxic CO to nontoxic CO₂ is the major function of the shifter, with a slight increase of hydrogen product. The byproduct CO₂ can be geologically stored in depleted natural gas reservoir to realize hydrogen production with zero carbon emission.

Equilibrium reactions are assumed in the reactors in this study to evaluate mass budget. Future work may introduce dynamic reactions to investigate how performance is affected by realistic reaction conditions in time series. Besides, numerical optimization can be further conducted to find optimal parameters for the reactors in the next-step work.

Acknowledgements

The financial support of the study is from grant #RC/RG-DVC/WRC/21/02 funded by Oman Ministry of Higher Education, Research and Innovation, and grant #IG/DVC/WRC/22/02 funded by Sultan Qaboos University (SQU). We also appreciate research group #DR/RG/17 at SQU for its technical support.

Conflict of interest

The authors declare no competing interest.

Open Access This article is distributed under the terms and conditions of the Creative Commons Attribution (CC BY-NC-ND) license, which permits unrestricted use, distribution, and reproduction in any medium, provided the original work is properly cited.

References

- Ansari, D. The hydrogen ambitions of the Gulf States: Achieving economic diversification while maintaining power. Paper Presented at SWP Comment, German Institute for International and Security Affairs, July, 2022.
- AspenTech. Aspen HYSYS V12.2, Bedford, MA 01730, USA, 2022.
- Ball, M., Weeda, M. The hydrogen economy-vision or reality? *International Journal of Hydrogen Energy*, 2015, 40(25): 7903-7919.
- Balta, M. T., Dincer, I., Hepbasli, A. Potential methods for geothermal-based hydrogen production. *International Journal of Hydrogen Energy*, 2010, 35(10): 4949-4961.
- Bicer, Y., Dincer, I. Development of a new solar and geothermal based combined system for hydrogen production. *Solar Energy*, 2016, 127: 269-284.
- Bühlmann, P. Bagging, subbagging and bragging for improving some prediction algorithms, in *Recent Advances and Trends in Nonparametric Statistics*, edited by M. G. Akritas, D. N. Politis, and Greenwich, USA, pp. 9-34,

- 2003.
- Cancela, A., Sanchez, A., Maceiras, R., et al. Simulation of natural gas steam reforming to obtain high-purity hydrogen. *Chemistry and Technology of Fuels and Oils*, 2015, 51: 529-535.
- Chen, M., Abdalla, O. A., Izady, A., et al. Development and surrogate-based calibration of a CO₂ reservoir model. *Journal of Hydrology*, 2020, 586: 124698.
- Chen, M., Al-Maktoumi, A., Izady, A. Assessment of integrated CO₂ geologic storage and geothermal harvest in a semi-closed thin reservoir. *Sustainable Energy Technologies and Assessments*, 2022, 49: 101773.
- Chen, M., Sun, Y., Fu, P., et al. Surrogate-based optimization of hydraulic fracturing in pre-existing fracture networks. *Computers & Geosciences*, 2013, 58: 69-79.
- Chiu, Y., Chiu, H., Hsieh, R.-H., et al. Simulations of hydrogen production by methanol steam reforming. *Energy Procedia*, 2019, 156: 38-42.
- Friedman, J. H. Multivariate adaptive regression splines. *Annals of Statistics*, 1991, 19(1): 1-67.
- Hermesmann, M., Müller, T. E. Green, turquoise, blue, or grey? Environmentally friendly hydrogen production in transforming energy systems. *Progress in Energy and Combustion Science*, 2022, 90: 100996.
- Hjeij, D., Biçer, Y., Koç, M. Hydrogen strategy as an energy transition and economic transformation avenue for natural gas exporting countries: Qatar as a case study. *International Journal of Hydrogen Energy*, 2022, 47(8): 4977-5009.
- Ihoeghian, N. A., Oyinkuro, K. C., Osagiede, C. A., et al. Steady-state simulation and optimization of hydrogen production by steam reforming of natural gas. *Journal of Nigerian Association of Mathematical Physics*, 2018, 44: 323-330.
- Inayat, A., Raza, M., Khan, Z., et al. Flowsheet modeling and simulation of biomass steam gasification for hydrogen production. *Chemical Engineering & Technology*, 2020, 43(4): 649-660.
- [Mathworks. MatLab & Simulink: Simulink Reference R2022b, 2022.](#)
- McKay, M. D., Beckman, R. J., Conover, W. J. A comparison of three methods for selecting values of input variables in the analysis of output from a computer code. *Technometrics*, 1979, 21(2): 239-245.
- Mokheimer, E. M. A., Hussain, M. I., Ahmed, S., et al. On the modeling of steam methane reforming. *Journal of Energy Resources Technology*, 2015, 137(1): 012001.
- Mostafaeipour, A., Khayyami, M., Sedaghat, A., et al. Evaluating the wind energy potential for hydrogen production: A case study. *International Journal of Hydrogen Energy*, 2016, 41(15): 6200-6210.
- Peng, X., Jin, Q. Molecular simulation of methane steam reforming reaction for hydrogen production. *International Journal of Hydrogen Energy*, 2022, 47(12): 7569-7585.
- Picard, R. R., Cook, R. D. Cross-validation of regression models. *Journal of the American Statistical Association*, 1984, 79: 575-583.
- Pourali, M., Esfahani, J. A., Sadeghi, M. A., et al. Simulation of methane steam reforming in a catalytic micro-reactor using a combined analytical approach and response surface methodology. *International Journal of Hydrogen Energy*, 2021, 46(44): 22763-22776.
- Razavi, S., Tolson, B. A., Burn, D. H. Review of surrogate modeling in water resources. *Water Resources Research*, 2012, 48(7): W07401.
- Saleem, M. S., Abas, N., Kalair, A. R., et al. Design and optimization of hybrid solar-hydrogen generation system using TRNSYS. *International Journal of Hydrogen Energy*, 2020, 45(32): 15814-15830.
- Sandler, S. I. *Chemical and Engineering Thermodynamics (Third Edition)*. Hoboken, US, John Wiley & Sons, 1999.
- Scovell, M. D. Explaining hydrogen energy technology acceptance: A critical review. *International Journal of Hydrogen Energy*, 2022, 47(19): 10441-10459.
- Seyitoglu, S. S., Dincer, I., Kilicarslan, A. Energy and exergy analyses of hydrogen production by coal gasification. *International Journal of Hydrogen Energy*, 2017, 42(4): 2592-2600.
- Sobol', I. M. Global sensitivity indices for nonlinear mathematical models and their Monte Carlo estimates. *Mathematics and Computers in Simulation*, 2001, 55(1-3): 271-280.
- Ulleberg, Ø. Modeling of advanced alkaline electrolyzers: A system simulation approach. *International Journal of Hydrogen Energy*, 2003, 28(1): 21-33.
- Veziroglu, T. N., Sahin, S. 21st century's energy: Hydrogen energy system. *Energy Conversion and Management*, 2008, 49(7): 1820-1831.
- Yue, M., Lambert, H., Pahon, E., et al. Hydrogen energy systems: A critical review of technologies, applications, trends and challenges. *Renewable and Sustainable Energy Reviews*, 2021, 146: 111180.
- Zhang, T., Liu, J., Sun, S. Technology transition from traditional oil and gas reservoir simulation to the next generation energy development. *Advances in Geo-Energy Research*, 2023, 7(1): 69-70.
- Zhang, T., Zhang, Y., Katterbauer, K., et al. Phase equilibrium in the hydrogen energy chain. *Fuel*, 2022, 328(15): 125324.